

*Water Science and Engineering*, Mar. 2008, Vol. 1, No. 1, 27–36  
ISSN 1674–2370, <http://kbb.hhu.edu.cn>, e-mail: [wse@hhu.edu.cn](mailto:wse@hhu.edu.cn)

# Effects of storm waves on rapid deposition of sediment in the Yangtze Estuary channel

Xu Fumin<sup>\*1,2</sup>, Zhang Changkuan<sup>1</sup>, Mao Lihua<sup>1</sup>, Tao Jianfeng<sup>1</sup>

1. Key Laboratory of Coastal Disaster and Defence of Ministry of Education, Hohai University, Nanjing 210098, P. R. China

2. College of Ocean, Hohai University, Nanjing 210098, P. R. China

**Abstract:** Recent research on short-term topographic change in the Yangtze Estuary channel under storm surge conditions is briefly summarized. The mild-slope, Boussinesq and action balance equations are compared and analyzed. The action balance equation, SWAN, was used as a wave numerical model to forecast strong storm waves in the Yangtze Estuary. The spherical coordinate system and source terms used in the equation are described in this paper. The significant wave height and the wave orbital motion velocity near the bottom of the channel during 20 m/s winds in the EES direction were simulated, and the model was calibrated with observation data of winds and waves generated by Tropical Cyclone 9912. The distribution of critical velocity for incipient motion along the bottom was computed according to the threshold velocity formula for bottom sediment. The mechanism of rapid deposition is analyzed based on the difference between the root-mean-square value of the near-bottom wave orbital motion velocity and the bottom critical tractive velocity. The results show that a large amount of bottom sediments from Hengsha Shoal and Jiudian Shoal are lifted into the water body when 20 m/s wind is blowing in the EES direction. Some of the sediments may enter the channel with the cross-channel current, causing serious rapid deposition. Finally, the tendency of the storm to induce rapid deposition in the Yangtze Estuary channel zone is analyzed.

**Key words:** Yangtze Estuary; storm waves; action balance equation; wave orbital motion velocity near the bottom; bottom critical velocity; rapid deposition

## 1 Introduction

Waves are one of the main hydrodynamic forces in coastal zones. In the Yangtze Estuary (Figure 1), it is thought that the bottom sediments are lifted by wave action and transported by tidal current. Sediment transport in the estuary channel zone is closely related to storm waves. Waves in the shoal area that are strong enough to lift the bottom sediment cause large-scale fluid mud movement. The waves in the estuary are mainly wind waves and hybrid waves. Past experience shows that bed shear stress caused by waves generated by winds of Beaufort force 4 or 5 in the E or S direction is equivalent to that caused by the spring tide in the flood season (Xu et al. 1989; Gu 1986). There is even greater erosion when the spring tide and the tropical cyclone happen to take place at the same time, causing serious sediment deposition in the channel. Although the storms do not remain in a fixed place for a long period of time, a large amount of sediments leave the shoal bed and a thick layer of fluid mud forms on the channel bed, leading to disasters for coastal engineering. It is reported that storm wave aggradation

---

This work was supported by the National Natural Science Foundation of China (Grant No. 50779015).

<sup>\*</sup>Corresponding author (e-mail: [fmxu@hhu.edu.cn](mailto:fmxu@hhu.edu.cn))

Received Jan. 17, 2008; accepted Feb. 23, 2008

accounts for 30% to 40% of the thickness of aggradational morphology in the Yangtze Delta. More than  $4 \times 10^6 \text{ m}^3$  of sediments were deposited in the Yangtze Estuary channel when Tropical Cyclone 8310 invaded the estuary zone (Xu et al. 1989). Fluid mud deposition with a thickness of 1.2 m covering the entire 28-km length of the Tongsha Channel was observed in the Yangtze Estuary in 1976 (Gu 1986).

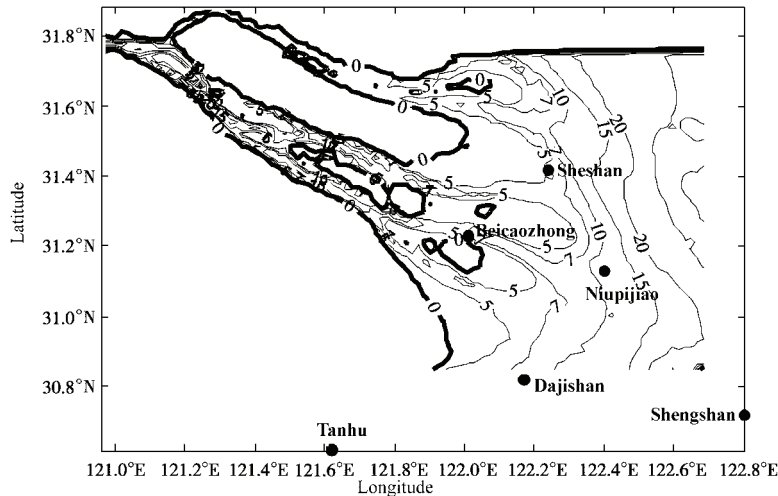


**Figure 1** The Yangtze Estuary and observation stations

(The isolines in the figure are water depth in m)

Many experts have paid a great deal of attention to the effects of storm surges on short-term topographic change in coastal areas. Ren et al. (1983) and Li et al. (1995) analyzed the effects of storm surges on the formation of tidal shoals on the coast of Jiangsu Province. Gu (1988) suggested that storm surges are one of the most important factors in riverbed evolvement in the Yangtze Estuary in his analysis of storm surge data in 1974. Engineers have observed rapid deposition on the riverbed during the tropical cyclone process in which sediment is deposited in the channel while the shoal surface erodes. However, the mechanisms of the storm waves' effect on rapid deposition are still not clear. Research is mainly focused on the abnormal variations of water level in the Yangtze Estuary resulting from storm surges; little research has been done on storm waves' contribution to the development of shoals and channels in the estuary zone. The fact is that the violent oscillatory motion of the water particles near the bottom under storm waves is large enough to lift a great amount of bottom sediments, even if the tidal current isn't considered. During a storm surge, the lifting of the fluid mud, newly deposited sediment and solid bed sediment are mainly caused by the strong current and the storm waves. Therefore, there is an urgent need for a better understanding of the effects of storm waves on rapid deposition in the Yangtze Estuary channel.

This paper proposes a numerical model suitable for forecasting storm waves in the estuary. Wave parameters in the channel zone such as the significant wave height and the wave orbital motion velocity near the bottom are numerically simulated. The influence of dynamic

storm waves on rapid deposition in the Yangtze Estuary channel is studied through analysis of the sediment's critical characteristics.

## 2 Numerical model for storm waves

Due to complicated topography and unsteady hydrodynamic conditions, accurately forecasting waves in the Yangtze Estuary remains a difficult problem. The mild-slope equation model (Berkhoff 1972; Radder 1979) is capable of simulating wave refraction, diffraction, reflection, bottom friction and wave breaking processes. However, this numerical method is based on the linear theory and can only describe the propagation process of mono-frequency waves. The Boussinesq equation (Nwogu 1993), which is a 2D nonlinear wave equation for shallow water, includes wave shoaling, refraction, diffraction and reflection processes, but is only suitable for a small-scale area. The action balance equation (Ris et al. 1994), which treats waves as an irregular random process, can reasonably describe wave shoaling, refraction, diffraction, bottom friction, wave breaking, whitecapping, wind energy input and nonlinear wave processes. Thus, it is applicable to large-, middle- and small-scale water areas. This wave model has been applied successfully, especially in forecasting wind waves in the surf zone, at coastal, estuary, offshore and ocean scales (Xu et al. 2000a, 2000b). In the Yangtze Estuary, trenches crisscross the shoals, storm waves and hybrid waves dominate, and strong nonlinear wave-wave interactions take place. The action balance equation is the most suitable model for forecasting storm waves in this area. In this study, the SWAN model, a third generation wave model based on the action balance equation, is used for typhoon-generated wave simulation.

### 2.1 Action balance equation in a spherical coordinate system

The spectrum in this model is the action density spectrum,  $N(\sigma, \theta)$ , rather than the energy density spectrum,  $E(\sigma, \theta)$ , since the action density, unlike the energy density, is conserved in the presence of a current field. The action density spectrum is expressed as

$$N(\sigma, \theta) = E(\sigma, \theta) / \sigma \quad (1)$$

In other words, the energy density spectrum is divided by the relative frequency,  $\sigma$ . The spectrum density may vary in time and space. In spherical coordinates, the spectral action balance equation is

$$\frac{\partial}{\partial t} N + \frac{\partial}{\partial \lambda} C_\lambda N + (\cos \varphi)^{-1} \frac{\partial}{\partial \varphi} C_\varphi \cos \varphi N + \frac{\partial}{\partial \sigma} C_\sigma N + \frac{\partial}{\partial \theta} C_\theta N = \frac{S}{\sigma} \quad (2)$$

The first term on the left side of this equation represents the local rate of change in the action density,  $N$ , over time; the second and third terms represent propagation of action density in the longitude,  $\lambda$ , and latitude,  $\varphi$ , directions, respectively; the fourth term represents the shifting of the relative frequency,  $\sigma$ , due to variations in depth and current; the fifth term represents propagation in  $\theta$  space, that is, the depth-induced and current-induced refraction;

$S$  on the right side is an energy-density-related source term that includes wave growth caused by wind, wave-wave interactions and wave energy dissipation due to bottom friction, whitecapping and wave breaking; and  $C_\lambda$ ,  $C_\phi$ ,  $C_\sigma$ , and  $C_\theta$  represent the wave propagation velocities in  $\lambda$ ,  $\phi$ ,  $\sigma$  and  $\theta$  spaces, respectively.

## 2.2 Description of source terms

This model applies the most advanced research achievements in wave theory. In accordance with previous data and past research in the Yangtze Estuary, the spectral wave energy input and output terms are calculated according to the following methods: the wind energy input term is based on the resonance mechanism of Phillips (Cavaleri and Malanotte-Rizzoli 1981) and the feedback mechanism of Miles (Komen et al. 1984); the bottom friction coefficient ranges from 0.004 to 0.008, which is consistent with many years of engineering research in the Yangtze Estuary (RICOE 1998); waves propagating from deep to shallow water lose energy due to depth-induced breaking, and the relationship between the maximum individual wave height,  $H_m$ , and the local depth,  $d$ , is

$$H_m = \gamma_b d \quad (3)$$

where  $\gamma_b$  is a breaker parameter defined as 0.73; the process of whitecapping is represented by the phase-based model of Hasselmann (1974), in which a wave number is used to describe energy dissipation due to whitecapping; the Discrete Iterative Approximation (DIA) method (Hasselmann et al. 1985) is used to compute quadruplet wave-wave interactions in deep or intermediate water depth; and the representation of the process of triad wave-wave interactions in very shallow water is based on the research of Abreu et al. (1992).

## 3 Model verification

Tropical Cyclone 9912 was first recorded on the ocean surface 550 kilometers east of Taiwan Island on September 19, 1999. Its wind reached a maximum value of over 48 m/s on September 22. The tropical cyclone landed in Nagasaki, Japan on September 24. The winds observed at observation stations in the Yangtze Estuary are shown in Table 1 (QOUOFCS 2000). The observed wave data at Sheshan station (122°14.4'E, 31°25.3'N) and Niupijiao station (122°15'E, 31°8'N) are shown in Table 2 and Table 3.

**Table 1** Observed winds of Tropical Cyclone 9912 in the Yangtze Estuary m/s

Date	Sheshan station			Dajishan station		
	Wave direction	Average wind velocity	Maximum wind velocity	Wave direction	Average wind velocity	Maximum wind velocity
1999-09-21	N	15.3	20.0	N-NNW	16.1	18.7
1999-09-22	N-NNE	17.0	21.7	N-NNE	18.2	23.0
1999-09-23	NNE	15.5	18.7	N-NNE	17.8	21.0
1999-09-24	N-NNE	8.7	20.0	NW-NNW	9.3	17.7

Using the daily average wind speed and wind direction in the estuary as the input for the simulation, significant wave height,  $H_{1/3}$ , and mean wave period,  $\bar{T}$ , were computed. The results are shown in Table 2 and Table 3.

**Table 2** Comparison between wave observation and the simulation results at Sheshan station

Date	Wave direction	Daily average values (observation data)		Daily average values (simulation data)	
		$H_{1/3}$ (m)	$\bar{T}$ (s)	$H_{1/3}$ (m)	$\bar{T}$ (s)
1999-09-21	N	1.9	4.8	1.9	4.1
1999-09-22	NNE	2.4	5.0	2.5	4.8
1999-09-23	NNE	2.1	5.2	2.4	6.0
1999-09-24	N-NE	1.6	5.9	1.4	6.5

**Table 3** Comparison between wave observation and simulation results at Niupijiao station

Date	Wave direction	Daily maximum values (observation data)		Daily maximum values (simulation data)	
		$H_{1/3}$ (m)	$\bar{T}$ (s)	$H_{1/3}$ (m)	$\bar{T}$ (s)
1999-09-21	N-NNW	1.8	4.9	2.0	4.7
1999-09-22	N-NNE	2.1	5.6	2.4	5.8
1999-09-23	N-NNE	2.3	5.6	2.5	5.9
1999-09-24	N-NW	1.5	6.0	1.8	6.5

## 4 Numerical simulation of storm waves in the Yangtze Estuary deep channel

Water depth data from the deep channel zone are obtained from the Yangtze Estuary marine chart of 1997. The mean water level is 2.22 m. A coordinate (120°58'E, 30°0.5'N) is defined as the origin of the computational domain, the E direction is defined as the  $x$  direction and the N direction is defined as the  $y$  direction. The cell size in both the  $x$  and  $y$  directions is 0.5'. The computational domain is 1°43' long in the  $x$  direction and 30' long in the  $y$  direction. The JONSWAP spectrum and four-order cosine function are applied to define the input 2D wave spectrum. The input wind velocity is 20 m/s, according to the recorded maximum from observation data, and its direction is 157.5°. The spectral wave direction distribution in  $\theta$  space ranges from 67.5° to 247.5° in the counter-clockwise direction. The directional resolution is 3'. The computational range of spectral frequency,  $\sigma$ , is defined from 0.05 Hz to 1.2 Hz, the mesh number is 13 and the frequency distribution on the frequency axis is logarithmic. The model domain includes Xuliujing at the western boundary, Luhuaashan Island at the eastern boundary, the northern part of Lianxinggang at the northern boundary, and the connecting line between Luchaogang and Luhuaashan Island as the southern boundary. The connecting line from Luhuaashan to the north is defined as the eastern open boundary, and the

water depth there ranges from 30 m to 40 m. The open boundary conditions are obtained according to the SMB method.

#### 4.1 Significant wave height in the deep channel zone

Significant wave height in the deep channel zone of the Yangtze Estuary is simulated under the input conditions above. The origin coordinate of the output computational area is (121°41.5'E, 31°3.5'N), and the lengths in the  $x$  and  $y$  directions are 37.5' and 18', respectively. Significant wave height in the deep channel zone is shown in Figure 2, where the units are transformed from degrees to meters.

Figure 2 shows large significant wave heights in the channel zone downstream of Hengsha East Sandbank Deep Trench and the Flood Tidal Trench at Hengsha Shoal. The significant wave heights along most of Hengsha Shoal and Jiuduan Sandbank are over 2 m. There exists an obvious wave convergence phenomenon on the shoal and sandbank. Waves at Hengsha East Sandbank Deep Trench propagate from the south to the north. At west of Jiuduan Sandbank, where shoals crisscross trenches, the variation of wave directions is complex.

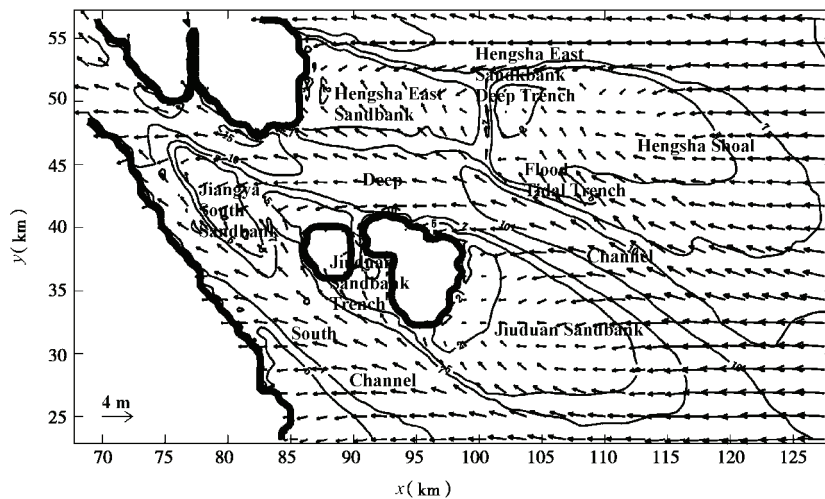


**Figure 2** The significant wave height field in the deep channel zone of the Yangtze Estuary

#### 4.2 Wave orbital motion velocity near the bottom in the deep channel zone

The root-mean-square value of wave orbital motion velocity near the bottom represents the waves' potential energy to lift the bottom sediments. Its physical meaning is therefore more obvious than wave height. For irregular random waves, the root-mean-square value of the wave orbital motion velocity near the bottom,

$$U_{\text{rms}} = \left( \sum_{i=1}^N U_i^2 \right)^{1/2} \quad (4)$$

can be expressed as

$$U_{\text{rms}}^2 = \int_0^\infty \int_0^{2\pi} \frac{\sigma^2}{\sinh^2(kd)} E(\sigma, \theta) d\theta d\sigma \quad (5)$$

where  $d$  is water depth,  $k$  is wave number,  $\sigma$  is angular frequency, and  $E(\sigma, \theta)$  is spectral density.

Figure 3 shows that all of the calculated root-mean-square values of near-bottom wave orbital motion velocity at Hengsha East Sandbank, Jiangya South Sandbank, Hengsha Shoal and Jiuduan Sandbank are over 0.3 m/s; values along large parts of Hengsha Shoal and Jiuduan Sandbank are between 0.4 m/s and 0.5 m/s; and values are about 0.2 m/s in the Hengsha East Sandbank Deep Trench, the scouring trough under the trench, the upper section of the deep channel, Jiangya North Channel and the scouring trough under the Jiuduan Sandbank Trench. This clearly indicates that the water particle vibration velocity caused by storm waves can easily lift fluid mud and bottom sediment in shoal and sandbank areas along the two sides of the deep channel. It also indicates that the waves' effect on shoals and sandbanks is larger than that on trenches and scouring troughs.

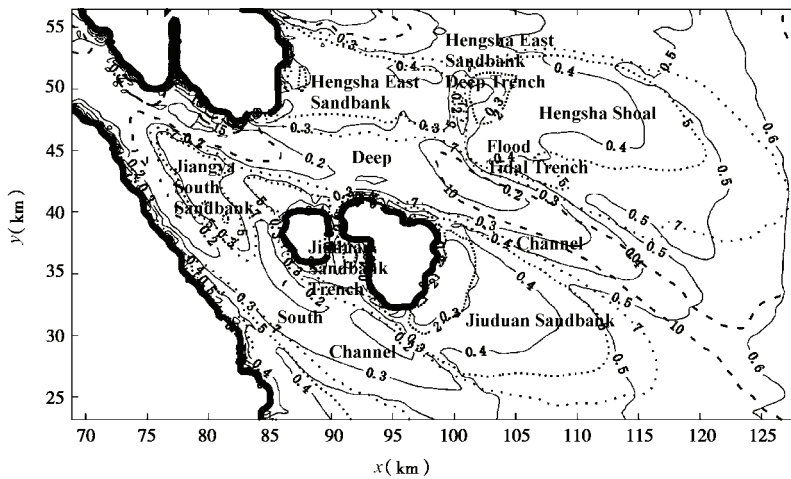


**Figure 3** Root-mean-square value field of the wave orbital motion velocity near the bottom of the Yangtze Estuary deep channel (unit: m/s)

## 5 Rapid deposition mechanism of the Yangtze Estuary deep channel under the influence of storm waves

The Yangtze Estuary is a muddy estuary. The sediment particles are fine and cohesive. Based on shallow drilling data from the estuary (RICOE 1998), the median diameter of sediment particle,  $d_{50}$ , ranges from 0.0045 mm to 0.2 mm. Under strong storm wave conditions, the shearing force on the surface of the bottom sediment layer increases, due to the combined actions of the bottom wave particle oscillations and the bottom currents. The

sediment is lifted into the water body when the sediment flocculation structure is torn up. For the newly deposited sediment that is not compressed into solid bed sediment, the cohesive force within sediment particles must be considered. The formula proposed by Wuhan Hydropower College (SPCCHI 1992) for critical tractive velocity,  $U_c$ , averaged along water depth, is as follows:

$$U_c = \left( \frac{h}{d_{50}} \right)^{0.14} \left( 17.6 \frac{\gamma_s - \gamma}{\gamma} d_{50} + 0.605 \times 10^{-6} \frac{10+h}{(d_{50})^{0.72}} \right)^{1/2} \quad (6)$$

where  $\gamma_s$  and  $\gamma$  are density of sediment and water, respectively,  $h$  is water depth, and  $d_{50}$  is median size of sediment. The formula for bottom critical velocity,  $U_{bc}$ , is

$$U_{bc} = \frac{7}{6} \left( \frac{d_{50}}{h} \right)^{1/6} U_c \quad (7)$$

If only wave action is taken into account, the bottom sediment is lifted when the root-mean-square value of the wave orbital motion velocity near the bottom is larger than the bottom critical tractive velocity.

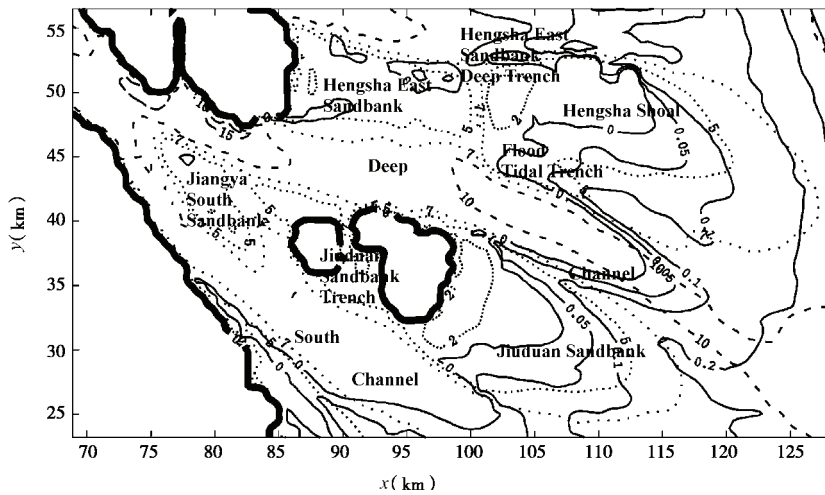


**Figure 4** Difference between the root-mean-square value of the orbital motion velocity near the bottom and bottom critical tractive velocity in the deep channel zone (unit: m/s)

Figure 4 shows that the root-mean-square values of orbital motion velocity near the bottom are larger than the bottom critical velocity at Hengsha Shoal, a large part of Jiuduankou Sandbank and some areas of Hengsha East Sandbank. The energy of storm waves acting on the shoals and sandbanks is strong enough to overcome the internal cohesive force of bottom sediments. The flocculation structure will be torn up and bottom sediment will be lifted into the water body. In fact, under these conditions, the fluid mud on the bottom is lifted before the bottom sediments.



## 6 Conclusions

The action balance equation, with a spherical coordinate system, was applied to the forecasting of storm waves in the Yangtze Estuary. The model was calibrated with field data observed during the tropical cyclone process. The significant wave height and the wave particle orbital motion velocity near the bottom of the deep channel zone were numerically simulated. The difference between the root-mean-square value of the orbital motion velocity near the bottom and bottom critical tractive velocity in the deep channel zone was computed according to the critical tractive velocity formula for bottom sediment.

Simulation results show that 20 m/s winds in the EES direction produce large significant wave heights in the channel zone beneath Hengsha East Sandbank Deep Trench, at Hengsha Shoal and along a large part of Jiudian Sandbank. The wave orbital motion velocity near the bottom is strong enough to lift the bottom sediment into the water body in the aforementioned area, even if the current is not taken into account. The results also indicate that the scour force in the shoal and sandbank zone is stronger than that in the deep trenches and troughs. It can be concluded that the effect of storm waves is to scour the shoal and sandbank and deposit sediment in the deep trenches and troughs. Wind conditions described in this paper are not extreme: the EES direction is not the most dangerous direction and 20 m/s is not the maximum wind velocity in the Yangtze Estuary channel. If the cyclone remains in the estuary for a long period of time, a great amount of sediment will be lifted and brought into the channel by the clockwise tidal current field and then become permanent deposition.

However, some problems remain to be solved: (1) During the process of erosion and deposition in the Yangtze Estuary, the fluid mud should be lifted first, followed by the newly deposited silt, and lastly the solid bed sediment. The bottom shearing forces created by storm waves are large enough to lift the sediment in a large part of the shoal and sandbank area, but the threshold property of solid bed sediments needs to be studied further. (2) A large belt of waves breaks in the Yangtze Estuary surf zone as a result of the strong wind storms and complicated topography. The short-term strong erosion due to wave breaking within this belt remains a difficult problem, and needs to be studied further. (3) The storm currents in the Yangtze Estuary are very strong. In addition, the tropical cyclone wind field is non-stationary; it varies dramatically in space and time. In order to forecast the process of rapid deposition, a coupled model, including storm waves, storm currents and tidal currents, should be developed in the future.

## References

- Abreu, M., Larraza, A., and Thornton, E. 1992. Nonlinear transformation of directional wave spectra in shallow water. *Journal of Geophysical Research*, 97(C10), 15579–15589.
- Berkhoff, J. C. W. 1972. Computation of combined refraction-diffraction. *Proc. 13th Coastal Engineering Conference*, Vancouver: American Society of Civil Engineers, 471–490.
- Cavaleri, L., and Malanotte-Rizzoli, P. 1981. Wind wave prediction in shallow water: Theory and applications.

- Journal of Geophysical Research*, 86(C11), 10961–10973.
- Gu, G. C. 1988. Preliminary analysis of the surge wave in the Yangtze River estuary: Dynamic and geomorphic processes. Shanghai: Shanghai Science and Technological Publishing Company. (in Chinese)
- Gu, W. H. 1986. Effect of Typhoon on the sedimentation in Tongsha dredged channel in Changjiang River Estuary. *Marine Sciences*, 10(1), 60–62. (in Chinese)
- Hasselmann, K. 1974. On the spectral dissipation of ocean waves due to white capping. *Boundary-Layer Meteorology*, 6(1–2), 107–127.
- Hasselmann, S., Hasselmann, K., Allender, J. H., and Barnett, T. P. 1985. Computations and parameterizations of the nonlinear energy transfer in a gravity-wave spectrum. Part II: Parameterizations of the nonlinear energy transfer for application in wave models. *Journal of Physical Oceanography*, 15(11), 1378–1391.
- Komen, G. J., Hasselmann, S., and Hasselmann, K. 1984. On the existence of a fully developed wind-sea spectrum. *Journal of Physical Oceanography*, 14, 1271–1285.
- Li, C. X., Zhang, G. J., and Li, T. S. 1995. Rhythms of tidal flat sedimentation and cyclicity of affecting factors. *Acta Sedimentologica Sinica*, 13(S), 71–78. (in Chinese)
- Nwogu, O. 1993. Alternative form of Boussinesq equations for nearshore wave propagation. *Journal of Waterway, Port, Coastal, and Ocean Engineering*, 119(6), 618–638.
- Qingdao Ocean University, Ocean Forecast Center of Shanghai (QOUOFCs). 2000. *Analysis report of waves in the Yangtze River Estuary*. (in Chinese)
- Radder, A. C. 1979. On the parabolic equation method for water-wave propagation. *Journal of Fluid Mechanics*, 95(1), 159–176.
- Ren, M. E., Zhang, R. S., Yang, J. H., and Zhang, D. C. 1983. The influence of storm tide on mud plain coast—With special reference to Jiangsu Province. *Marine Geology & Quaternary Geology*, 3(4), 1–24. (in Chinese)
- Research Institute of Coastal and Ocean Engineering (RICOE). 1998. Report on channel efficiency of sidecasting at the lower section of the deep navigation waterway in the Yangtze River Estuary. Nanjing: Hohai University. (in Chinese)
- Ris, R. C., Houlthuisen, L. H., and Booij, N. 1994. A spectral model for waves in the near shore zone. Edge, B. L., ed., *Proc. 24th International Coastal Engineering Conference*, 68–78. New York: American Society of Civil Engineers.
- Sediment Professional Committee of China Hydraulic Institute (SPCCHI). 1992. *Sediment Manual*. Beijing: China Environmental Science Publishing Company. (in Chinese)
- Xu, F. M., Yan, Y. X., Zhang, C. K., Song, Z. Y., and Mao, L. H. 2000a. Wave numerical model for shallow water. *China Ocean Engineering*, 14(2), 193–202.
- Xu, F. M., Zhang, C. K., Mao, L. H., and Song, Z. Y. 2000b. Application of a numerical model for shallow water waves. *Journal of Hydrodynamics*, Ser. A, 15(4), 429–434. (in Chinese)
- Xu, S. Y., Shao, X. S., Chen, Z. Y., and Yan, Q. S. 1989. Serial study of storm-caused deposition of the Yangtze River Delta. *China Science*, Series B, 19(7), 97–103. (in Chinese)